Bioscience Reports (2020) **40** BSR20194309
https://doi.org/10.1042/BSR20194309

PORTLAND PRESS

Research Article

MiR-30e-5p inhibits the migration and invasion of nasopharyngeal carcinoma via regulating the expression of MTA1

Weiqun Hu[1], Wenfeng Yao[2], Haolin Li[2] and Li Chen[3]

[1]Department of Otorhinolaryngology, The Affiliated Hospital of Putian University, China; [2]Department of Otorhinolaryngology, Xinxiang First People's Hospital, China; [3]Department of Otorhinolaryngology, Zaozhuang Municipal Hospital, China

Correspondence: Li Chen (lich_chenlil@163.com)

The study explored the effect of miR-30e-5p on nasopharyngeal carcinoma (NPC). MiR-30e-5p levels in NPC cancer and adjacent normal samples, in metastatic and non-metastatic cancer samples of NPC, and in NP69 cell and five NPC cell lines were determined by quantitative real-time polymerase chain reaction (qRT-PCR). The relationship between miR-30e-5p and MTA1 was confirmed by dual-luciferase reporter assay, Western blot and qRT-PCR. The viability, migration and invasion of 5-8F and 6-10B cells were determined by CCK-8, scratch test and transwell assays, respectively. The levels of migration-related proteins (vimentin and Snail) and invasion-related proteins (MMP2 and MMP3) in NPC cells were detected by Western blot. The results showed that low expression of miR-30e-5p was associated with HNSC cancer, NPC, metastasis of NPC and NPC cell lines. Overexpressed miR-30e-5p in HNSC cancer and NPC was predictive of a better prognosis of patients. In addition, the viability, migration and invasion were reduced by up-regulating miR-30e-5p in 5-8F cells, but promoted by down-regulated miR-30e-5p in 6-10B cells. MiR-30e-5p reversed the migration and invasion of NPC cells regulated by MTA1, and inhibited migration and invasion of NPC cells via regulating MTA1 expression.

Introduction

Nasopharyngeal carcinoma (NPC) is a highly invasive and frequently diagnosed cancer of the head and neck [1]. Apart from virus infections such as Epstein-Barr virus infection, environmental factors and genetic susceptibility contribute to NPC progression [2]. NPC rises from nasopharynx, and frequently invades to lymph nodes in the nearby region surrounding the neck [3]. Within the boundaries of the nasopharynx, NPC invades the adjacent anatomical spaces or organs of Rosenmuller's fossa, where the epicentre of the NPC often occurs [4]. Metastatic cancers impose more difficulties of treatment than non-metastatic ones [5]. Metastatic NPC greatly reduces the survival chance of advanced NPC patients [6]. Though early-staged and locally advanced NPC commonly have a good prognosis, for NPC patients with recurrence or metastasis, they have a median overall survival of about twenty months and also limited clinical options [7]. Surgical resection currently remains the main treatment for NPC patients with recurrence or metastasis [8]. Thus, the molecular mechanism of the metastasis of NPC cells should be explored so as to provide alternative strategies for the management of the cancer.

MiRNAs are a class of endogenous small non-coding genes that primarily exert its effects on post-transcriptional regulation and different biological processes [9]. Abnormally expressed miRNAs play pivotal roles in the development of many human cancers [10,11]. Dysregulated miRNAs in most cancers

Received: 12 December 2019
Revised: 14 April 2020
Accepted: 21 April 2020

Accepted Manuscript online: 07 May 2020
Version of Record published: 27 May 2020

Bioscience Reports (2020) **40** BSR20194309
https://doi.org/10.1042/BSR20194309

Table 1 The relationship between miR-30e-5p and clinical characteristics of NPC patients

Characteristics	No. of patients ($n = 62$)	No. of patients		*P*
		miR-30e-5p low group	miR-30e-5p high group	
Age (years)				0.301
≤45	30	18	12	
>45	32	15	17	
Gender				0.773
Male	35	17	16	
Femal	29	16	13	
TNM stage				0.003
I+II	22	6	16	
III+IV	40	27	13	
Local or distant metastasis				0.000
No	27	5	22	
Yes	35	28	7	

induce the dysregulation of normal regulatory networks by functioning as tumor suppressors or oncogenes [12]. Mature miRNAs modulate the processes of gene expressions through targeting the 3′ untranslated regions (3′UTR) of downstream mRNAs and restraining protein translation or initiating mRNA degradation of many mRNA transcripts [13]. These molecules typically reduce the stability of mRNAs, including certain genes mediating tumorigenesis such as apoptosis and invasion [14].

Studies have demonstrated that miRNAs has diagnostic and therapeutic values for many cancers [15–17]. MiR-30e-5p, which is a newly cancer-related miRNA, plays a pivotal role in the progression of different cancers, such as in non-small cell lung cancer [18], colorectal cancer [19], bladder cancer [20]. However, the functional role of miR-30e-5p in NPC is less reported.

The present study first found that miR-30e-5p expression was closely related to metastasis and prognosis of NPC. As we went on investigating the effects of miR-30e-5p on NPC progression of NPC, we found its downstream target gene MTA1 and underlying mechanisms in NPC cells. The present findings provide a novel molecular target and related mechanisms for NPC treatment.

Materials and methods

Clinical specimens

Six-two NPC and adjacent normal samples were obtained from the Affiliated Hospital of Putian University between 02/14/2017 and 02/14/2019. All the patients were pathologically diagnosed as NPC, and no patients had received radiotherapy or chemotherapy before the surgery. All the patients signed the written informed consent before the surgery, and Research Ethics Committee of the Affiliated Hospital of Putian University (AHPU20170114342) permitted our study according to the Declaration of Helsinki [21]. The clinicopathological features of NPC patients are shown in Table 1.

Cell culture

Human immortalized nasopharyngeal epithelial cell line (NP69) and five human NPC cell lines (5-8F, SUNE1, C666, 6-10B and HK1) were purchased from Shanghai Institute of Biological Sciences (Shanghai, China). All human NPC cells were cultivated in RPMI Medium 1640 (31800, Solarbio, China) with 10% fetal bovine serum (FBS). The NP69 cell was cultivated in serum-free medium (12753018, ThermoFisher, U.S.A.) containing all necessary growth factors (Gibco). In addition, 5-8F cell has highly tumorigenic and metastatic, and 6-10B cell has tumorigenic ability but lacks metastatic ability [22]. All the cells were maintained in an environment with 95% humidity and 5% CO_2 at 37°C.

Cell transfection

Before transfection, 5-8F and 6-10B cells (2.5×10^4/well) were cultivated in six-well plates for 24 h. For miRNA transfection, miR-30e-5p mimics (miR10000692-1-5) and inhibitor (miR20000692-1-5), and the mimic control (miR1190315051351), inhibitor control (miR2N0000001-1-5) were purchased from RiboBio (Guangzhou, China).

Table 2 Primer sequences used for quantitative real-time polymerase chain reaction (qRT-PCR)

Genes		Primer sequences(5 -3)
miR-30e-5p	Forward	GGGTGTAAACATCCTTGAC
	Reverse	TGCGTGTCGTGGAGTC
MTA1	Forward	GACCAGGCAGGCTTTCTATC
	Reverse	CTG TTGATGGGCAGGTAGG
U6	Forward	CTCGCTTCGGCAGCACA
	Reverse	AACGCTTCACGAATTTGCGT
GADPH	Forward	GCTTCGGCAGCACATATACTAAAAT
	Reverse	CGCTTCACGAATTTGCGTGTCAT

For MTA1 transfection, MTA1 cDNA was amplified by PCR and constructed into pcDNA3.1 vector (V79020, ThermoFisher, U.S.A.) to generate pcDNA-AKT2 overexpression plasmid. The empty MTA1 vector was considered as a negative control (NC) of pcDNA-MTA1. MTA1 siRNA (siG000219854B-1-5) and siRNA NC (siN0000001-1-5) were obtained from RiboBio (Guangzhou, China). Before cell collection, all the vectors were transfected into NPC cells for 48 h to up-regulate or down-regulate the expression of miR-30e-5p or MTA1 in NPC cells using Lipofectamine® 2000 Transfection Reagent (11668, ThermoFisher, U.S.A.).

Targeted relationship prediction and dual-luciferase reporter assay

The potential relationship between miR-30e-5p and MTA1 was predicated using Targetscan7.2. The 3′UTR of MTA1 containing the predicted miR-30e-5p binding site was amplified by PCR and cloned into the downstream of the luciferase-coding sequence in the pGL3 (E1761, Promega, Madison, WI, U.S.A.) to form MTA1-wild-type (MTA1-WT) reporter vector. The putative binding site of miR-30e-5p in MTA1 was mutated using site-directed mutagenesis kit (Takara, Shiga, Japan), and the sequence of putative binding site was redefined as MTA1-mutated-type (MTA1-MUT).

NPC cells were co-transfected with the MTA1-WT or MTA1-MUT, and miR-30e mimics (5-8F cells), or inhibitor (6-10B cells) using Lipofectamine® 2000 Transfection Reagent. After transfection for 48 h, the cells were lysed and the relative luciferase activities of these cells were detected using Dual-Luciferase® Reporter Assay System (E1910, Promega). Firefly luciferase was normalized to Renilla luciferase for individual well.

Quantitative real-time polymerase chain reaction (qRT-PCR)

Total RNAs were extracted from the cells or NPC tissues and corresponding normal tissues using TRIzol® Reagent (15596018, ThermoFisher, U.S.A.). For miRNA analysis, reverse transcription reaction and qRT-PCR of miR-30e-5p were performed by Hairpin-it ™ microRNA and U6 snRNA Normalization RT-PCR Quantitation Kit (E22001-E22010, GenePharma, Shanghai, China) in 7500 Fast Real-Time PCR System (Applied Biosystems, U.S.A.). The reaction parameters were set as follows: at 95°C for 3 min, 40 cycles at 95°C for 12 s, and at 62°C for 40 s. For the analysis of mRNA expressions, reverse transcription was performed by PrimeScript™ RT reagent Kit with gDNA Eraser (RR047A, Takara, Japan). QRT-PCR was performed in 7500 Fast Real-Time PCR System (Applied Biosystems, Foster City, CA, U.S.A.) using TB Green® Premix Ex Taq™ II (RR820Q, Takara). Conditions were set as follows: a predenaturation at 95°C for 30 min, followed by 40 cycles at 95°C for 5 s and at 60°C for 30 s, followed by melt curve conditions at 95°C for 5 s, at 60°C for 1 s, and annealing at 50°C for 30 s. MiR-30e-5p and MTA1 levels were respectively normalized to U6 snRNA (U6, E22001-E22010, GenePharma) and GAPDH levels by the $2^{-\triangle\triangle CT}$ method [23]. GAPDH was synthetized by Sangon Biotech. The sequences of primers used are listed in Table 2.

Cell counting kit-8 (CCK-8) assay

The cell viability was measured by CCK-8 (CA1210, Solarbio) following the manufacturer's protocol. The NPC cells (1×10^3/well) were cultivated on 96-well plates for 24, 48, and 72 h, and added with CCK-8 solution (10 μl) for cultivation for another 4 h. Finally, the absorbance was determined at 450 nm by a microplate reader (SpectraMax iD5, Molecular Devices, U.S.A.).

Scratch wound healing assay

The 5-8F (2.5×10^4/well) and 6-10B cells (2.5×10^4/well) were cultured to 80–90% confluence in the six-well plates. The medium was discarded, confluent 5-8F and 6-10B were scratched using a 10 μl tip, washed by serum-free RIPM

Bioscience Reports (2020) **40** BSR20194309
https://doi.org/10.1042/BSR20194309

1640 medium, and incubated for 48 h. Cell migration was examined by counting migrated cells from five random fields of each chamber under a 100× inverted microscope (Ts2r-FL, Nikon, Japan). The following formula [(1 – the distance following healing/the distance prior to healing) × 100%] was used to calculated relative migration rates of 5-8F and 6-10B cells.

Transwell assay

Cell invasion of 5-8F and 6-10B cells was assessed by transwell chambers (8-μm pores, Corning Inc., Corning, U.S.A.) coated with Matrigel gel (BD Biosciences, San Jose, CA). The 5-8F and 6-10B cells (1×10^5/cells) were cultivated into the upper chambers of Transwell (Corning Inc., Corning, U.S.A.), which contained 200 μl DMEM, while 500 μl DMEM medium containing 10% FBS was added into the lower wells as the primers. After 48 h at 37°C, 5-8F and 6-10B cells remaining in the upper surface were scraped off by a cotton swab, while those migrated into the lower surface were fixed by 4% pre-cold methanol for 15 min, and stained by 0.1% Crystal Violet solution (Sigma-Aldrich) for 20 min at room temperature. The cells were counted from a minimum of 10 fields per filter under a 200× microscope (Ts2r-FL, Nikon, Japan).

Western blot assay

Lysates of 5-8F and 6-10B cells were quickly lysed for protein isolation, and the expressions of migration-related proteins (vimentin and Snail), invasion-related proteins (MMP2 and MMP3) and MTA1 protein were determined. The total proteins were extracted from 5-8F and 6-10B cells using RIPA buffer (R0010, Solarbio) with a complete protease inhibitor cocktail (539133, Merck) and reacted on ice for 30 min. Next, the supernatants were collected and the protein concentration of supernatants was measured by BCA protein assay kit (Solarbio).

After protein centrifugation and quantification, the supernatants (30 μg/lane) were separated on 6–24% SDS-PAGE gels for protein detection, and the proteins were transferred onto polyvinylidene difluoride membranes (PVDF, Millipore Corp. Bedford, MA, U.S.A.). Subsequently, the membranes were blocked by 5% (w/v) skimmed milk for 1 h under 37°C, and then exposed to the specific primary antibodies [anti-vimentin (Rabbit, 1:1000, ab92547, Abcam, U.S.A.); anti-Snail antibody (Goat, 1:500, ab53519, Abcam, U.S.A.); anti-MMP2 (Rabbits, 1:2000, ab37150, Abcam, U.S.A.); anti-MMP3 (Rabbit, 1:1000, ab52915, Abcam, U.S.A.); anti-MTA1 (Rabbit, 1:2000, ab71153, Abcam, U.S.A.); anti-GAPDH antibody (Mouse, 1:500, ab8245, Abcam, U.S.A.)] at 4°C overnight, with the same species IgG used as the internal control. Next, the membranes were incubated with HRP-conjugated secondary antibody (Goat Anti-Mouse, 1:2000, ab205719, Abcam, U.S.A.), HRP-conjugated secondary antibody (Goat Anti-Rabbit, 1:2000, ab205718, Abcam, U.S.A.) and HRP-conjugated secondary antibody (Donkey Anti-Goat, 1:2000, ab205723, Abcam, U.S.A.) at 37°C for 2 h, and then washed three times at an interval of 10 min. Finally, specific protein signals were developed by ECL detection kit (ECL, Premega, U.S.A.), and target bands was visualized by ImageJ software (Image J 1.8.0, National Institute of Health).

Statistical analysis

The data were shown as mean ± standard deviation (S.D.). Chi-square test was used to determine the correlation between miR-30e-5p and clinical features of NPC patients. The significant difference between cancer and normal samples of HNSC was analyzed by StarBase v3.0 project. Kaplan–Meier plots were plotted by log-Rank test. Paired *t*-test was performing for comparison of paired samples. The comparison between two different groups was performed by Student's *t* test, while comparisons among multiple groups were conducted by one-way ANOVA analysis of variance followed by Bonferroni *post hoc test*. A $P<0.05$ was considered to be a statistical significance, and analyses were performed using SPSS 17.0 software (SPSS, Inc., Chicago, IL, U.S.A.).

Results

Low expression of miR-30e-5p was related to the adverse clinicopathological features of NPC patients

NPC patients were divided into two groups according to the cut-off value, which was defined as the median value of the miR-30e-5p expression as follows: miR-30-5p low expression group (lower than the median level, $n = 33$) and miR-30e-5p high expression group (higher than the median level, $n = 29$). No statistically significant differences were found in age and gender between miR-30e-5p low expression and miR-30e-5p high expression groups (Table 1, $P > 0.05$), suggesting that the data had comparative significance. As shown in Table 1, low-expressed miR-30e-5p was obviously associated with more advanced tumor-node-metastasis (TNM) stage ($P = 0.003$) and with the occurrence

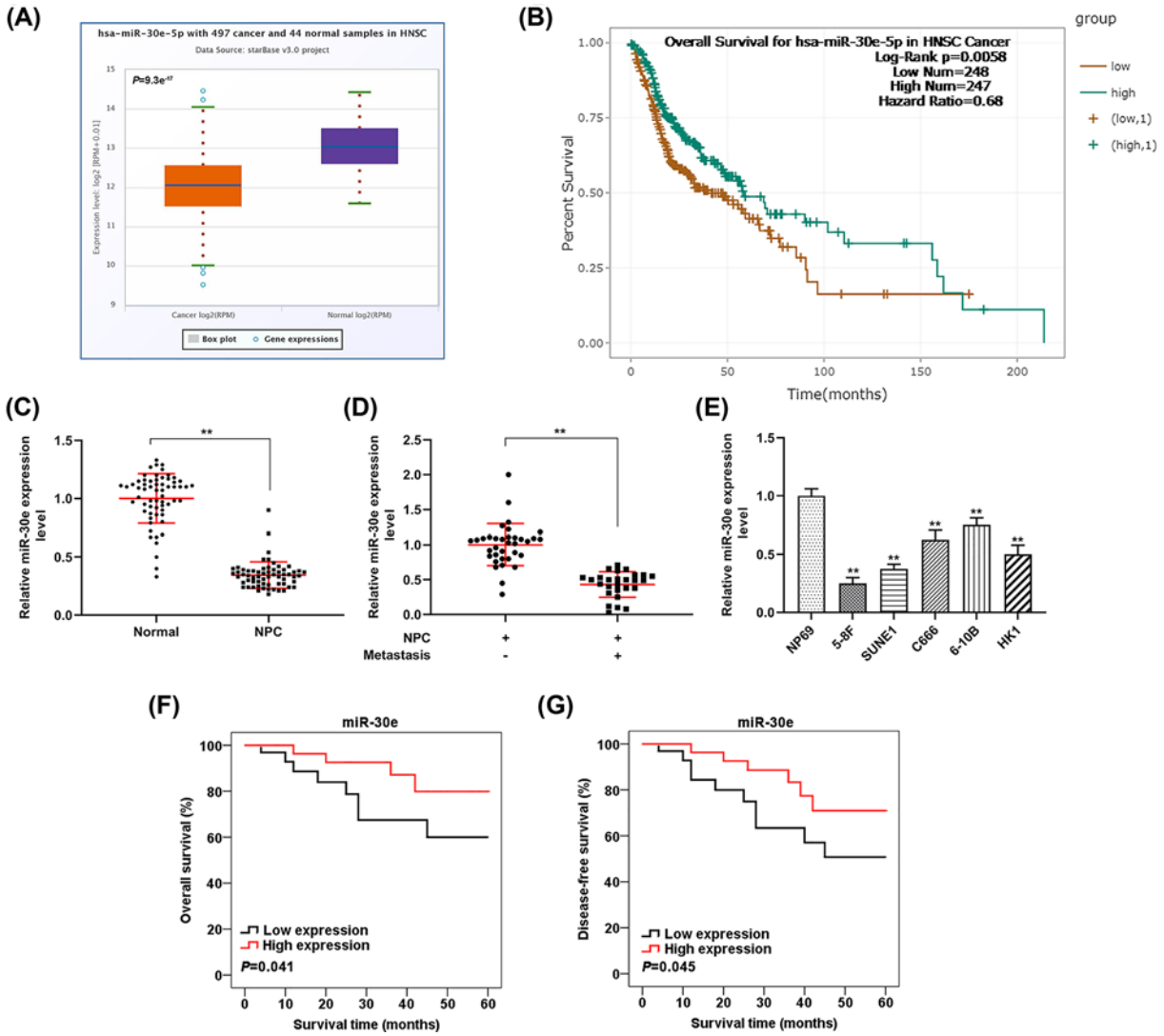

Figure 1. The miR-30e-5p expression in tissues and cells of nasopharyngeal carcinoma (NPC) was detected

(**A**) MiR-30e-5p with differential expression in normal samples and cancer of head and neck squamous cell (HNSC) was predicted by StarBase v3.0 project. (**B**) Overall survival for miR-30e-5p in HNSC cancer was predicted by log-rank test. (**C**) MiR-30e-5p expression was detected by quantitative real-time polymerase chain reaction (qRT-PCR) in NPC tissues and normal tissues; $^{**}P<0.01$ vs. Normal. (**D**) MiR-30e-5p expression was detected by qRT-PCR in NPC tissues with or without metastasis; $^{**}P<0.01$ vs. NPC without metastasis. (**E**) MiR-30e-5p expression in five NPC cell lines and NP69 cell line was detected by qRT-PCR; $^{**}P<0.01$ vs. NP69. (**F**) The relationship between miR-30e-5p expression and overall survival of NPC patients was analyzed by Kaplan–Meier. (**G**) The relationship between miR-330e expression and disease-free survival of NPC patients was analyzed by Kaplan–Meier. U6 was used as internal reference. The data were shown as mean ± standard deviation (S.D.).

of metastasis of NPC ($P<0.001$). The clinical data revealed that low-expressed miR-30e-5p was related to the adverse clinicopathological features of NPC patients.

The expression level of miR-30e-5p in NPC tissues and cells

StarBase v3.0 predicted that miR-30e-5p was differentially expressed in cancer ($n = 497$) and normal samples ($n = 44$), and that miR-30e-5p expression was reduced in HNSC cancer samples (Figure 1A, $P = 9.3e^{-17}$). Moreover, the data revealed that the survival chance of HNSC patients in miR-30e-5p high expression group was significantly higher than those in miR-30e-5p low expression group, suggesting that high-expressed miR-30e-5p is predictive of a better prognosis of HNSC (Figure 1B, $P = 0.0058$). To validate the prediction, the level of miR-30e-5p expression

Bioscience Reports (2020) **40** BSR20194309
https://doi.org/10.1042/BSR20194309

in clinical samples obtained from NPC patients was determined by qRT-PCR, and the result showed that expression of miR-30e-5p was obviously reduced in NPC tissues than that in normal tissues (Figure 1C, $P<0.01$), and the most obvious reduction was found in NPC tissues with metastasis (Figure 1D, $P<0.01$). Moreover, miR-30e-5p expression was reduced in five NPC cells line compared with the NP69 cell line (Figure 1E, $P<0.01$). The data suggested that miR-30e-5p functioned as tumor-suppressor in NPC progression and was involved in the metastasis of NPC.

Kaplan–Meier plots showed that overall survival rates of NPC patients in miR-30e-5p high expression group and miR-30e-5p low expression group was 79.9 % and 60.0 %, respectively (Figure 1F, $P = 0.041$), and that disease-free survival rates in miR-30e-5p high expression group and miR-30e-5p low expression group was 71.0 % and 50.7 %, respectively (Figure 1G, $P = 0.045$). These findings showed that higher expression of miR-30e-5p was predictive of a better prognosis of NPC patients, which was consistent with the result of overall survival for miR-30e-5p in HNSC cancer.

MiR-30e-5p inhibited the viability, migration and invasion of NPC cells

The functional effects of miR-30e-5p in NPC cells were investigated. We respectively transfected miR-30e-5p mimic and inhibitor into 5-8F and 6-10B cells to investigate the role of miR-30e-5p in NPC progression.

The qRT-PCR data demonstrated that miR-30e-5p mimic significantly increased the miR-30e-5p expression in 5-8F cells (Figure 2A, $P<0.01$). Three time points (24, 48 and 72 h) were determined for cell viability experiments for confirming the time point when miR-30e-5p mimic exerted effects on cell viability. CCK-8 assay showed that increased miR-30e-5p expression significantly reduced viability of 5-8F cells at 48 and 72 h (Figure 2C, $P<0.05$).

Scratch and transwell experiments showed that up-regulated miR-30e-5p obviously suppressed migration (Figure 2E,F, $P<0.01$) and invasion (Figure 2H,J, $P<0.05$) of 5-8F cells.

To further verify the effect of miR-30e-5p on the viability, migration and invasion of NPC cells, miR-30e-5p expression was down-regulated in the cells using miR-30e-5p inhibitor. The qRT-PCR experiment showed that miR-30e-5p inhibitor obviously reduced miR-30e-5p expression of 6-10B cells (Figure 2B, $P<0.05$). Down-regulation of miR-30e-5p obviously reduced cell viability at 48 and 72 h. (Figure 2D, $P<0.05$), and significantly increased migration (Figure 2E,G, $P<0.05$) and invasion (Figure 2I,J, $P<0.01$) of 6-10B cells.

MiR-30e-5p inhibited the levels of migration-related and invasion-related proteins of NPC cells

In consistent with the results of migration and invasion assays, Western blot assay showed that increasing miR-30e-5p expression obviously decreased relative expressions of migration-related proteins (vimentin and Snail) and invasion-related proteins (MMP-2 and MMP-3) of 5-8F cells (Figure 3A, $P<0.05$ or $P<0.01$), while reducing miR-30e-5p expression significantly increased relative expressions of migration-related proteins (vimentin and Snail) and invasion-related proteins (MMP-2 and MMP-3) of 6-10B cells (Figure 3B, $P<0.01$).

MiR-30e-5p directly regulated MTA1 expression in NPC cells

To explain the underlying molecular mechanism about the functional effect of miR-30e-5p in NPC cells, we used bioinformatics methods to identify the downstream target of miR-30e-5p. Targetscan7.2 found that MTA1 had possible binding sites in miR-30e-5p (Figure 4A), and dual-luciferase reporter verified that miR-30e-5p could bind to the 3′UTR of MTA1. We observed that up-regulated miR-30e-5p obviously reduced the luciferase activity of MTA1-MT (Figure 4B, $P<0.01$), but did not affect that of the MTA1-MUT (Figure 4B). Moreover, down-regulation of miR-30e-5p significantly increased the luciferase activity of MTA1-MT (Figure 4C, $P<0.01$), whereas that of MTA1-MUT was not affected (Figure 4C).

QRT-PCR and Western blot assays were performed to further explore the interaction between miR-30e-5p and MTA1 of NPC cells, and the data revealed that up-regulated miR-30e-5p obviously decreased the mRNA and protein expressions of MTA1 of the 5-8F cells (Figure 4D,E, $P<0.01$), while down-regulation of miR-30e-5p obviously increased the mRNA and protein expression of MTA1 of the 6-10B cells (Figure 4F,G, $P<0.01$). The data demonstrated that MTA1 not only was a downstream target of miR-30e-5p, its expression was directly regulated by miR-30e-5p in NPC cells.

MiR-30e-5p completely reversed the effect of MTA1 on migration and invasion of NPC cells

The effect of MTA1 on 5-8F and 6-10B cells was explored to further invesitgate whether MTA1 was a functional mediator of miR-30e-5p in NPC cells. The data showed that compared with negative control (NC) group, MTA1

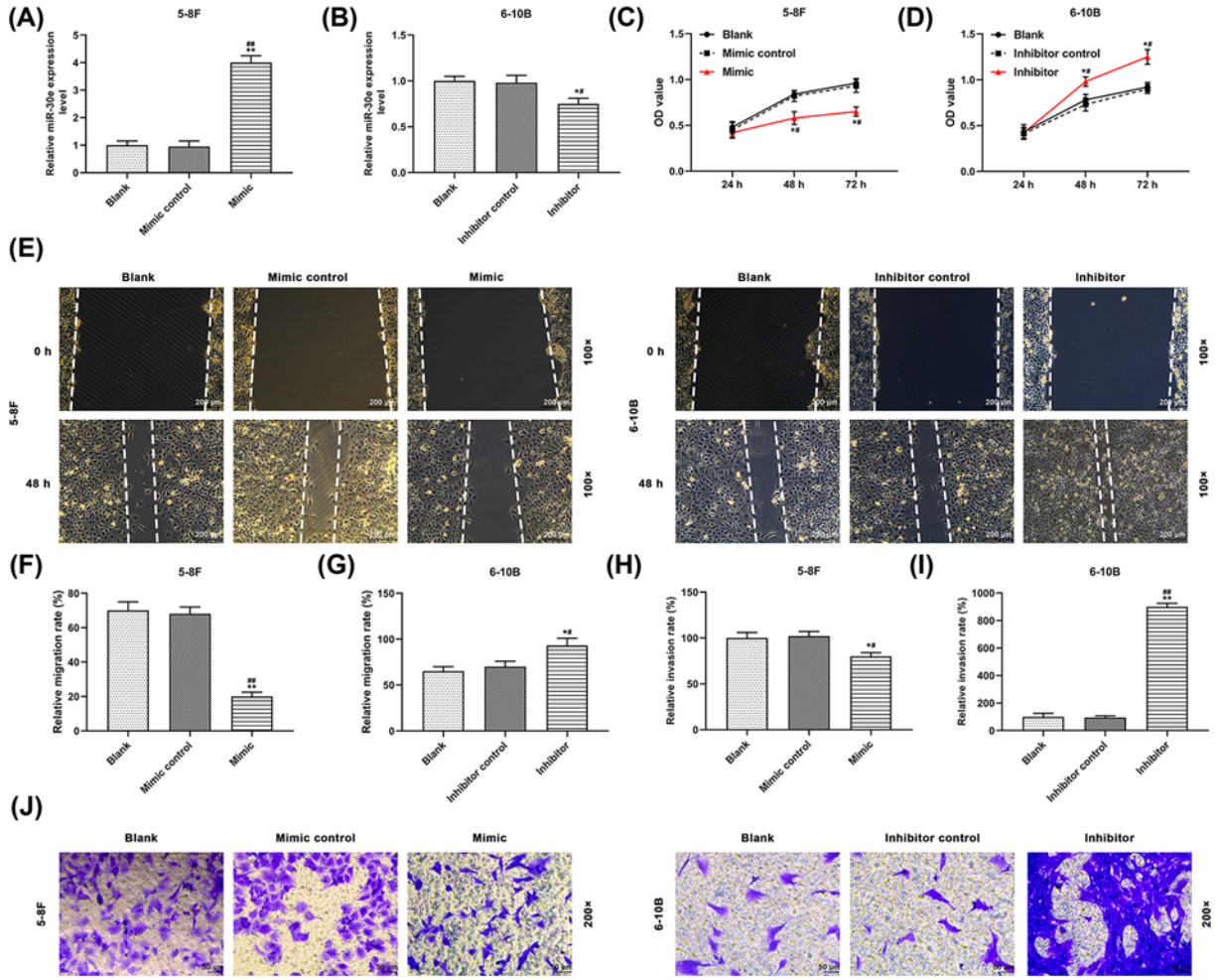

Figure 2. MiR-30e-5p inhibited the viability, migration and invasion of NPC cells

(**A**) Transfection efficiency of miR-30e-5p mimic into 5-8F cells was determined by quantitative real-time polymerase chain reaction (qRT-PCR); $^{**}P<0.01$ vs. Blank, $^{\#\#}P<0.01$ vs. Mimic control. (**B**) Transfection efficiency of miR-30e-5p inhibitor in 6-10B cells was determined by qRT-PCR; $^{*}P<0.05$ vs. Blank, $^{\#}P<0.05$ vs. Inhibitor control. The effects of miR-30e-5p mimic on viability (**C**), migration (**E** and **F**) and invasion (**H** and **J**) of 5-8F were determined by CCK-8 assay, scratch test and transwell assay, respectively; $^{*}P<0.05$, $^{**}P<0.01$ vs. Blank, $^{\#}P<0.05$, $^{\#\#}P<0.01$ vs. Mimic control. The effects of miR-30e-5p inhibitor on viability (**D**), migration (**E** and **G**) and invasion (**I** and **J**) of 6-10B cells were determined by CCK-8 assay, scratch test and transwell assay, respectively; $^{*}P<0.05$, $^{**}P<0.01$ vs. Blank, $^{\#}P<0.05$, $^{\#\#}P<0.01$ vs. Inhibitor control. The data were shown as mean ± standard deviation (S.D.).

expression of 5-8F cells was obviously increased in MTA1 group (Figure 5A, $P<0.01$), while MTA1 expression of 5-8F cells was obviously decreased in miR-30e-5p mimic (Mimic) + NC group (Figure 5A, $P<0.01$). MTA1 expression of Mimic + MTA1 group was obviously lower than that of MTA1 group (Figure 5A, $P<0.05$), but obviously higher than that of Mimic + NC group in 5-8F cells (Figure 5A, $P<0.01$). In contrast, compared with siRNA negative control (siNC) group, level of MTA1 expression of 6-10B cells was significantly reduced in siMTA1 group (Figure 5B, $P<0.01$), while that in miR-30e-5p inhibitor (Inhibitor) + NC group was significantly increased (Figure 5B, $P<0.01$). Moreover, the level of MTA1 expression of 6-10B cells in Inhibitor + siMTA1 group was observed higher compared with that in siMTA1 group (Figure 5B, $P<0.05$), but was obviously lower compared with that in Inhibitor + NC group (Figure 5B, $P<0.01$).

From migration and invasion experiments, we found that migration and invasion rates of the NCP cells were significantly increased by MTA1 transfection (Figure 5C, E–G, $P<0.05$ or $P<0.01$), which was significantly reversed by miR-30e-5p mimic in 5-8F cells (Figure 5C,E–G, $P<0.01$). Moreover, migration and invasion of 6-10B cells were significantly decreased by siMTA1 transfection (Figure 5D,E,F,H, $P<0.05$, $P<0.01$), but obviously reversed by

Bioscience Reports (2020) **40** BSR20194309
https://doi.org/10.1042/BSR20194309

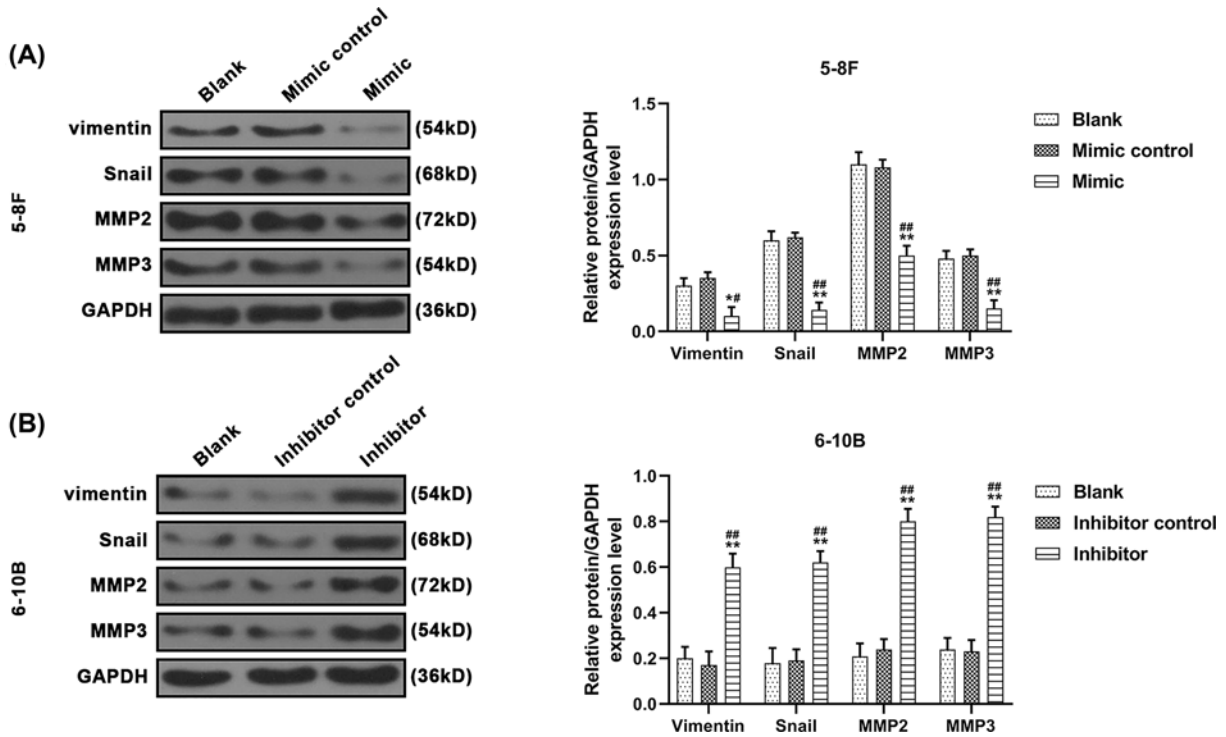

Figure 3. The expression levels of migration- and invasion-related proteins in 5-8F and 6-10B cells

(**A**) The levels of migration-related proteins (vimentin and Snail) and invasion-related proteins (MMP2 and MMP3) in 5-8Fcells were determined by Western blot assay; $^{*}P<0.05$, $^{**}P<0.01$ vs. Blank, $^{\#}P<0.05$, $^{\#\#}P<0.01$ vs. Mimic control. (**B**) The levels of migration-related proteins (vimentin and Snail) and invasion-related proteins (MMP2 and MMP3) in 6-10B cells were determined by Western blot assay; $^{**}P<0.01$ vs. Blank, $^{\#\#}P<0.01$ vs. Inhibitor control. GAPDH was used as internal reference. The data were shown as mean ± standard deviation (S.D.).

miR-30e-5p inhibitor (Figure 5D–F,H, $P<0.05$, $P<0.01$). Taken together, these data demonstrated that miR-30e-5p suppressed migration and invasion of NPC by negatively regulating MTA1 expression.

MiR-30e-5p completely reversed the effect of MTA1 on migration and invasion-related proteins of NPC cells

The data showed that compared with negative control (NC) group, levels of migration-related proteins (vimentin and Snail) and invasion-related proteins (MMP-2 and MMP-3) were obviously increased in MTA1 group of 5-8F cells, and noticeably reduced in miR-30e-5p mimic (Mimic) + NC group (Figure 6A, $P<0.01$). Levels of migration-related proteins (vimentin and Snail) and invasion-related proteins (MMP-2 and MMP-3) in Mimic + MTA1 group were obviously lower than those in MTA1 group (Figure 6A, $P<0.01$). In contrast, compared with siRNA negative control (siNC) group, levels of migration-related proteins (vimentin and Snail) and invasion-related proteins (MMP-2 and MMP-3) in siMTA1 group were significantly decreased in 6-10B cells, while those of miR-30e-5p inhibitor (Inhibitor) + NC group were greatly increased (Figure 6B, $P<0.01$). Moreover, levels of migration-related proteins (vimentin and Snail) and invasion-related proteins (MMP-2 and MMP-3) of 6-10B cells in Inhibitor + siMTA1 group were higher compared with those of siMTA1 group (Figure 6B, $P<0.01$).

Discussion

Eighty-six thousand and five hundred patients were diagnosed with NPC in 2012 worldwide, and 71% of new cases occurred in East and Southeast Asia [24]. NPC showed high incidence and mortality China in 2013, bringing the need for disease control and prevention [25]. Though significant progress has been made in the treatment of NPC, the long-term prognosis of NPC patients is not satisfactory [7].

At present, targeted molecular therapies are seen as promising strategies for treating NPC, with fewer side effects compared with traditional treatments [26]. MiRNAs act as therapeutic targets and biomarkers for diagnosis and

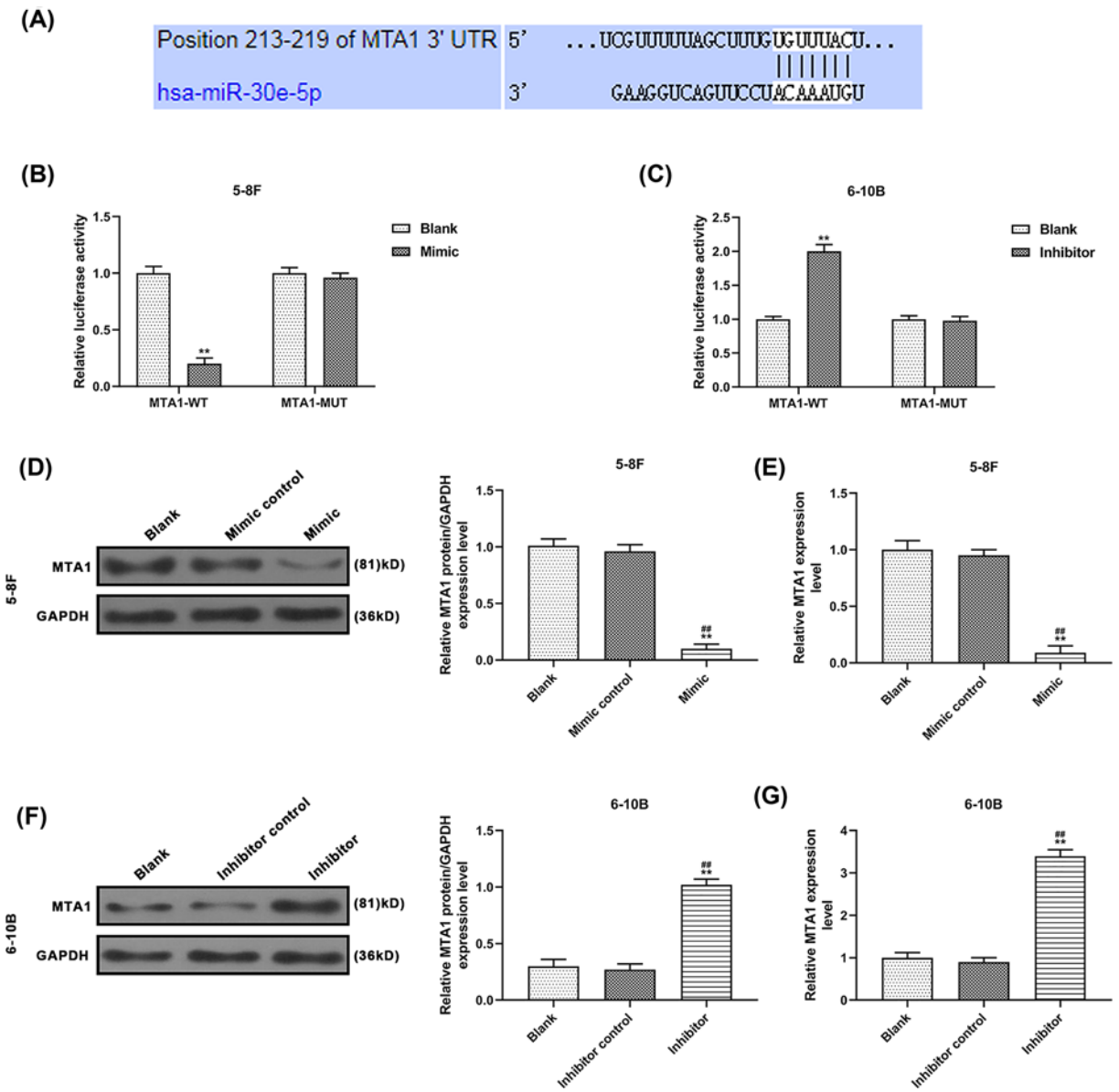

Figure 4. MiR-30e-5p directly regulated MTA1 expression in NPC cells

(**A**) Prediction of MTA1 contained a target site for miR-30e-5p by Targetscan7.2. (**B** and **C**) Dual-luciferase reporter assay showed that MTS1 was a target of miR-30e-5p. The relative MTA1 protein (**D**) and relative MTA1 expression (**E**) levels in 5-8F cells were determined by quantitative real-time polymerase chain reaction (qRT-PCR) and Western blot assays, respectively; $^{**}P<0.01$ vs. Blank, $^{\#\#}P<0.01$ vs. Mimic control. The relative MTA1 protein (**F**) and relative MTA1 expression (**G**) levels in 6-10B cells were determined by qRT-PCR and Western blot assays, respectively; $^{**}P<0.01$ vs. Blank, $^{\#\#}P<0.01$ vs. Inhibitor control. GAPDH was used as internal reference. The data were shown as mean ± standard deviation (S.D.).

prognosis of human cancers [27]. By starBase prediction in HNSC cancer samples and conducting qRT-PCR assay on NPC clinical tissues and cell lines, the present study found that low-expressed miR-30e-5p was related to more advanced TNM stage and metastasis of the NPC patients, while high-expressed miR-30e-5p was predictive of a better prognosis of the patients. The data above revealed that miR-30e-5p acted as a tumor suppressor and biomarkers for diagnosis and prognosis of NPC progression, suggesting that miR-30e-5p might be a potential therapeutic target for the treatment of metastatic NPC.

To confirm whether miR-30e-5p functioned as a novel effective target during NPC progression, we investigated its effect on cell viability, migration and invasion of 5-8F and 6-10B cells. The data above have revealed the relationship

Bioscience Reports (2020) **40** BSR20194309
https://doi.org/10.1042/BSR20194309

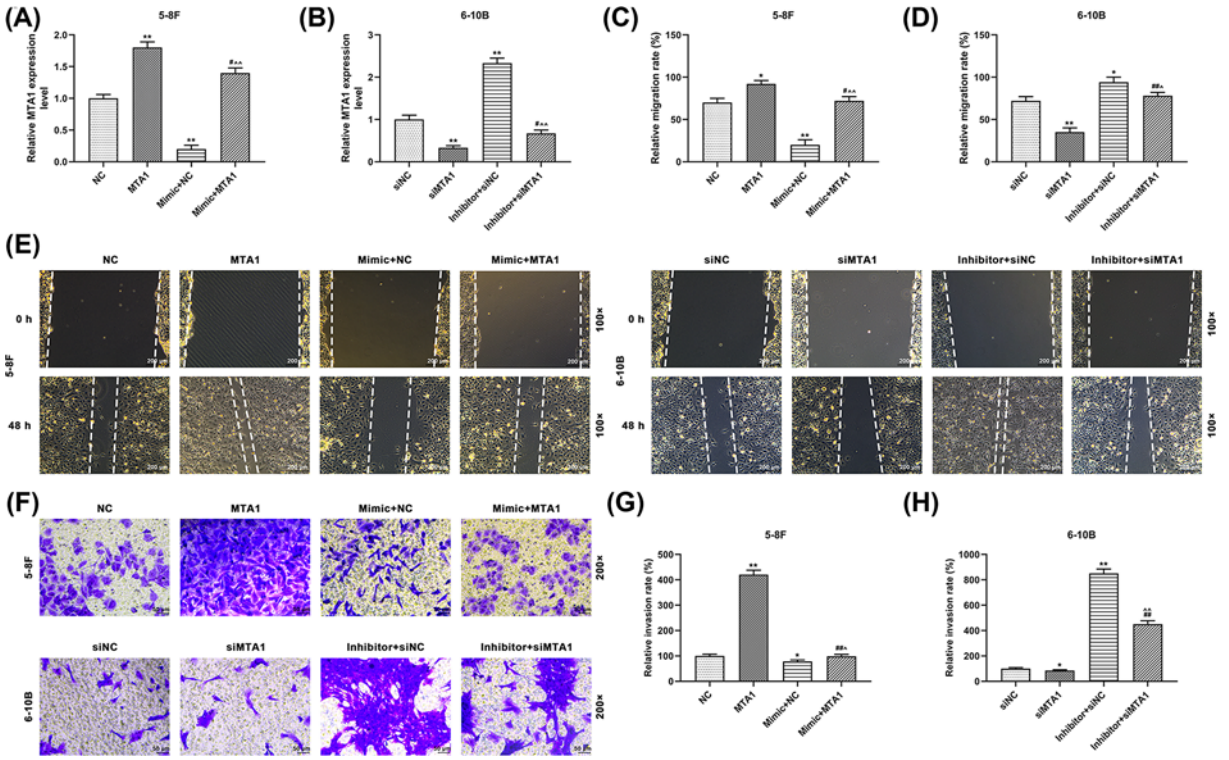

Figure 5. MiR-30e-5p completely reversed the effect of MTA1 on migration and invasion of NPC cells

(**A**) Relative TA1 expression levels of NC, MTA1, Mimic + NC and Mimic + MTA1 groups in 5-8F cells were determined by quantitative real-time polymerase chain reaction (qRT-PCR); $^{**}P<0.01$ vs. NC, $^{\#}P<0.05$ vs. MTA1, $^{\wedge\wedge}P<0.01$ vs. Mimic + NC. (**B**) Relative MTA1 expression levels of siNC, siMTA1, Inhibitor + siNC, and Inhibitor + siMTA1 groups in 6-10B cells were determined by qRT-PCR; $^{**}P<0.01$ vs. siNC, $^{\#}P<0.05$ vs. siMTA1, $^{\wedge\wedge}P<0.01$ vs. Inhibitor + siNC. (**C** and **E**) Relative migration rates of 5-8F cells in NC, MTA1, Mimic + NC, and Mimic + MTA1 groups were determined by scratch test; $^{*}P<0.05$, $^{**}P<0.01$ vs. NC, $^{\#}P<0.05$ vs. MTA1, $^{\wedge\wedge}P<0.01$ vs. Mimic + NC. (**D** and **E**) Relative migration rates of 6-10B cells in siNC, siMTA1, Inhibitor + siNC, and Inhibitor + siMTA1 groups were determined by scratch test; $^{*}P<0.05$, $^{**}P<0.01$ vs. siNC, $^{\#\#}P<0.01$ vs. siMTA1, $^{\wedge}P<0.05$ vs. Inhibitor + siNC. (**E**) The migration distance in 5-8F and 6-10 cells were pictured under an inverted microscope. (**F** and **G**) Relative invasion rates of NC, MTA1, Mimic + NC and Mimic + MTA1 groups in 5-8F cells were determined by transwell assay; $^{*}P<0.05$, $^{**}P<0.01$ vs. NC, $^{\#\#}P<0.01$ vs. MTA1, $^{\wedge}P<0.05$ vs. Mimic + NC. (**F** and **H**) Relative invasion rates of 6-10B cells in siNC, siMTA1, Inhibitor + siNC and Inhibitor + siMTA1 groups were determined by transwell assay; $^{*}P<0.05$, $^{**}P<0.01$ vs. siNC, $^{\#\#}P<0.01$ vs. siMTA1, $^{\wedge\wedge}P<0.01$ vs. Inhibitor + siNC. GAPDH was used as internal reference. (**A**, **C** and **G**) $^{*}P<0.05$, $^{**}P<0.01$ vs. NC, $^{\#}P<0.05$, $^{\#\#}P<0.01$ vs. MTA1, $^{\wedge}P<0.05$, $^{\wedge\wedge}P<0.01$ vs. Mimic + NC. (**B**, **D** and **H**) $^{*}P<0.05$, $^{**}P<0.01$ vs. siNC, $^{\#}P<0.05$, $^{\#\#}P<0.01$ vs. siMTA1, $^{\wedge}P<0.05$, $^{\wedge\wedge}P<0.01$ vs. Inhibitor + siNC. The data were shown as mean ± standard deviation (S.D.).

between miR-30e-5p and metastasis of NPC, and also suggested that miR-30e-5p suppressed the development of NPC by preventing the metastasis of NPC cells. Abnormal proliferation plays an important role in cancerization, and NPC is primarily biologically characterized by local invasion and distant metastasis [28]. Migration commonly refers to any directed cell movement within the body, and invasion of carcinomas signifies cell penetration across tissue barriers [29]. Migration and invasion of cancer cells allow the detachment from the primary tumor site and the spread of cancer within tissues [30]. Researchers have reported that miR-30e-5p is involved in the migration and invasion of different types of cancer. Zhang et al. indicated that cell proliferation and migration of bladder cancer are suppressed by miR-30e-5p [20]. MiR-30e-5p is induced by P53 to inhibit invasion and metastasis of colorectal cancer [19]. In this research, we found that overexpression of miR-30e-5p inhibited the viability, migration and invasion of 5-8F cells, but also reduced the expression levels of migration- and invasion-related proteins of 5-8F cells, while miR-30e-5p knockdown promoted the viability and migration and invasion of 6-10B cells, but also reduced the expression levels of migration- and invasion-related proteins of 6-10B cells. The data supported that miR-30e-5p functioned as a potential tumor suppressor in inhibiting the viability and metastasis of NPC cells. Consistent with our findings, a recent study also showed that miR-30e-5p suppressed proliferation and metastasis of NPC cells [28].

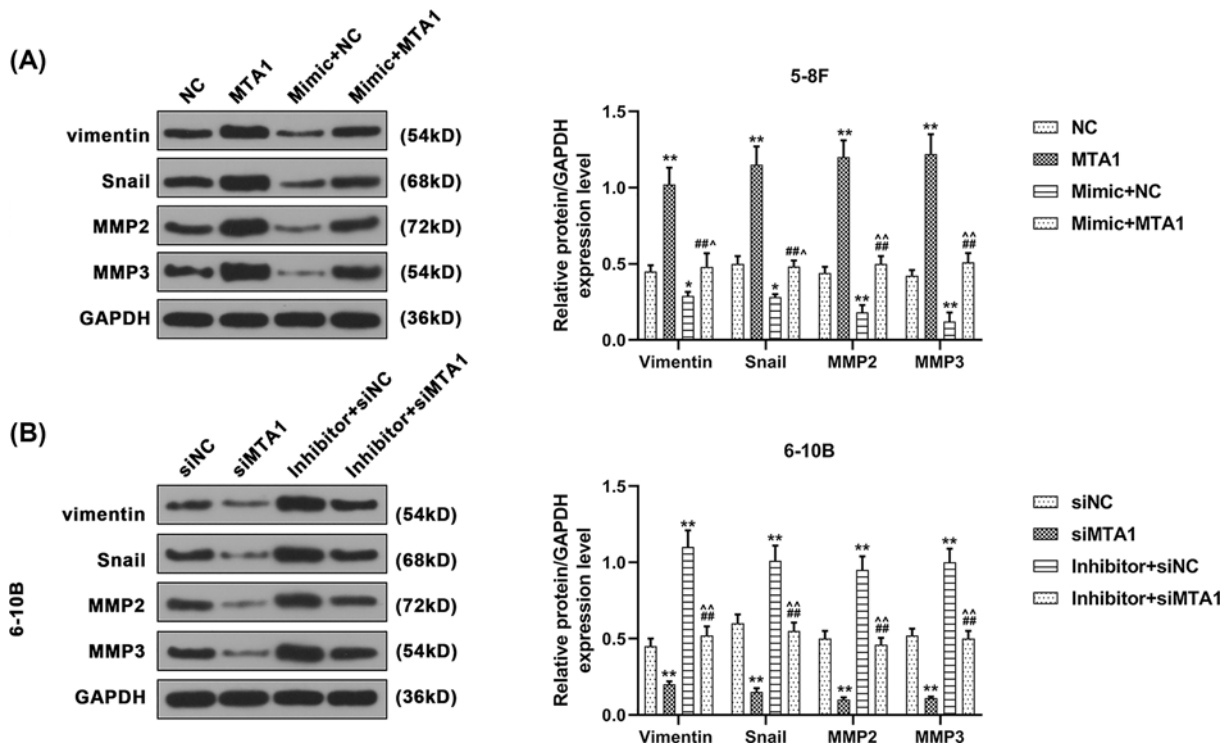

Figure 6. MiR-30e-5p completely reversed the effect of MTA1 on migration and invasion-related proteins of NPC cells

(**A**) The levels of migration-related proteins (vimentin and Snail) and invasion-related proteins (MMP2 and MMP3) in 5-8Fcells were determined by Western blot assay; $^{*}P<0.05$, $^{**}P<0.01$ vs. NC, $^{\#\#}P<0.01$ vs. MTA1, $^{\wedge}P<0.05$, $^{\wedge\wedge}P<0.01$ vs. Mimic+NC. (**B**) The levels of migration-related proteins (vimentin and Snail) and invasion-related proteins (MMP2 and MMP3) in 6-10B cells were determined by Western blot assay; $^{*}P<0.05$, $^{**}P<0.01$ vs. siNC, $^{\#\#}P<0.01$ vs. siMTA1, $^{\wedge}P<0.05$, $^{\wedge\wedge}P<0.01$ vs. Inhibitor+siNC. GAPDH was used as internal reference. The data were shown as mean ± standard deviation (S.D.).

MiRNAs mainly exert their biological effects through modulating target genes [31]. Targetscan7.2. predicted that MTA1 is a potential target gene of miR-30e-5p in NPC cells, and the prediction was further verified by dual-luciferase reporter assay, qRT-PCR and WWestern blot analysis. Previous study demonstrated that miR-30e-5p regulates MTA1 transcription through binding to its 3′-untranslated region in hepatocellular carcinoma [32]. Metastasis-associated gene 1 (MTA1), a component of histone deacetylase 1 involved in chromatin remodeling, is first cloned from the highly metastatic and non-metastatic rat mammary adenocarcinoma cell line using differential cDNA library screening [33]. MTA1, a cancer progression-related gene product, was correlated with tumorigenesis including invasion and metastasis [34]. MTA1 promotes NPC growth *in vitro* and *in vivo* [35]. MTA1 served as a novel biomarker for indicating metastatic potential of NPC, and also as a possible therapeutic target for the treatment of NPC with metastasis [36]. The current findings extended previous observations about the effect of AMTA1 on NPC development; moreover, we also found that the change of MTA1 expression reversed the functional effect of miR-30e-5p on the metastasis of NC cells, suggesting that MTA1 is also a functional downstream mediator of miR-30e-5p in NPC cells. Similar research has reported that MTA1 targeted by miR-183 overexpression to inhibit tumorigenesis of NPC [37].

Our findings demonstrated that miR-30e-5p expression could improve the prognosis of NPC by preventing metastasis of NPC, and further revealed underlying molecular mechanism of miR-30e-5p in suppressing the progression of NPC cells through the inhibition of MTA1 expression. Vimentin is a cellular-adhesion molecule in cell migration and invasion processes of tumor cells [38]. Vimentin promotes NPC cell migration and invasion [39]. High expression of epithelial-to-mesenchymal transition (EMT) marker Snail is indicative of high metastatic potential in NPC [40]. The inhibition of MMP2 was associated with the inhibition of NPC cell metastasis [41]. Tumor cell migration could be stimulated by MMP3 secretion in NPC tumor cells [42], In our study, miR-30e-5p inhibited the expressions of vimentin, Snail, MMP2 and MMP3, and promoted cell migration and invasion inhibition, while the function of miR-30e-5p could be reversed by MTA1, indicating that the function of miR-30e-5p on cell migration and invasion of NPC cells might be related to migration-related factors (vimentin and Snail) and invasion-related factors (MMP2 and

MMP3). However, it was a limitation not investigating more markers such as E-cadherin, which is related to EMT, this is because attention was paid to migration-related factors (vimentin and Snail) and invasion-related factors (MMP2 and MMP3). Our study found that miR-30e-5p played a pivotal role in modulating the migration and invasion of NPC cells, suggesting that miR-30e-5p might be a potential therapeutic target for NPC patients with metastasis.

Conclusion

MiR-30e-5p acts as a tumor suppressor in the progression of NPC cells by exerting its effects on migration and invasion of NPC cells through direct targeting MAT1. The present study investigated the underlying molecular target and mechanism of NPC treatment, and provided a possible target for therapy of NPC patients. Moreover, the results of the present study will be further examined and verified by conducting *in vivo* experiment using rats.

Competing Interests

The authors declare that there are no competing interests associated with the manuscript.

Funding

The authors declare that there are no sources of funding to be acknowledged.

Author Contribution

Substantial contributions to conception and design: W.H., W.Y.; Data acquisition, data analysis and interpretation: W.H., H.L., Drafting the article or critically revising it for important intellectual content: W.Y., L.C.; Final approval of the version to be published: All authors, Agreement to be accountable for all aspects of the work in ensuring that questions related to the accuracy or integrity of the work are appropriately investigated and resolved: L.C.

Abbreviations

3′UTR, 3′ untranslated regions; CCK-8 , cell counting kit-8; EMT , epithelial-to-mesenchymal transition; MTA1, metastasis-associated gene 1; NPC, nasopharyngeal carcinoma; qRT-PCR, quantitative real-time polymerase chain reaction.

References

1 Wang, H., Chen, H., Zhou, H., Yu, W. and Lu, Z. (2017) Cyclin-Dependent Kinase Inhibitor 3 Promotes Cancer Cell Proliferation and Tumorigenesis in Nasopharyngeal Carcinoma by Targeting p27. *Oncol. Res.* **25**, 1431–1440, https://doi.org/10.3727/096504017X14835311718295

2 Fan, C., Tu, C., Qi, P., Guo, C., Xiang, B., Zhou, M. et al. (2019) GPC6 Promotes Cell Proliferation, Migration, and Invasion in Nasopharyngeal Carcinoma. *J. Cancer* **10**, 3926–3932, https://doi.org/10.7150/jca.31345

3 Yue, P.Y., Ha, W.Y., Lau, C.C., Cheung, F.M., Lee, A.W., Ng, W.T. et al. (2017) MicroRNA profiling study reveals miR-150 in association with metastasis in nasopharyngeal carcinoma. *Sci. Rep.* **7**, 12012, https://doi.org/10.1038/s41598-017-10695-2

4 Chua, M.L.K., Wee, J.T.S., Hui, E.P. and Chan, A.T.C. (2016) Nasopharyngeal carcinoma. *Lancet (London, England)* **387**, 1012–1024, https://doi.org/10.1016/S0140-6736(15)00055-0

5 Xiao, Z., Chen, M., Yang, J., Yang, C., Lu, X., Tian, H. et al. (2019) MTBP regulates migration and invasion of prostate cancer cells in vitro. *Nan Fang Yi Ke Da Xue Xue Bao = J. Southern Med. Univ.* **39**, 6–12

6 Jiang, C., Wang, H., Zhou, L., Jiang, T., Xu, Y. and Xia, L. (2017) MicroRNA-212 inhibits the metastasis of nasopharyngeal carcinoma by targeting SOX4. *Oncol. Rep.* **38**, 82–88, https://doi.org/10.3892/or.2017.5641

7 Perri, F., Della Vittoria Scarpati, G., Caponigro, F., Ionna, F., Longo, F., Buonopane, S. et al. (2019) Management of recurrent nasopharyngeal carcinoma: current perspectives. *OncoTargets Ther.* **12**, 1583–1591, https://doi.org/10.2147/OTT.S188148

8 Huang, J., Li, Q., Zheng, Y., Shen, J., Li, B., Zou, R. et al. (2014) Partial hepatectomy for liver metastases from nasopharyngeal carcinoma: a comparative study and review of the literature. *BMC Cancer* **14**, 818, https://doi.org/10.1186/1471-2407-14-818

9 Liu, W., Cui, Z. and Zan, X. (2018) Identifying cancer-related microRNAs based on subpathways. *IET Syst. Biol.* **12**, 273–278, https://doi.org/10.1049/iet-syb.2018.5025

10 Tutar, Y. (2014) miRNA and cancer; computational and experimental approaches. *Curr. Pharm. Biotechnol.* **15**, 429, https://doi.org/10.2174/1389201015050140828161335

11 Huang, Z., Zhu, D., Wu, L., He, M., Zhou, X., Zhang, L. et al. (2017) Six Serum-Based miRNAs as Potential Diagnostic Biomarkers for Gastric Cancer. *Cancer Epidemiol. Biomarkers Prevent. : A Pub. Am. Assoc. Cancer Res. Cosponsor. Am. Soc. Prevent. Oncol.* **26**, 188–196

12 Xu, Y.F., Li, Y.Q., Guo, R., He, Q.M., Ren, X.Y., Tang, X.R. et al. (2015) Identification of miR-143 as a tumour suppressor in nasopharyngeal carcinoma based on microRNA expression profiling. *Int. J. Biochem. Cell Biol.* **61**, 120–128

13 Morquette, B., Juzwik, C.A., Drake, S.S., Charabati, M., Zhang, Y., Lecuyer, M.A. et al. (2019) MicroRNA-223 protects neurons from degeneration in experimental autoimmune encephalomyelitis. *Brain : J. Neurol.* 1–17

14 Farazi, T.A., Spitzer, J.I., Morozov, P. and Tuschl, T. (2011) miRNAs in human cancer. *J. Pathol.* **223**, 102–115, https://doi.org/10.1002/path.2806

15 Nagaraj, A.B., Joseph, P. and DiFeo, A. (2015) miRNAs as prognostic and therapeutic tools in epithelial ovarian cancer. *Biomark. Med.* **9**, 241–257, https://doi.org/10.2217/bmm.14.108
16 Wen, Y., Han, J., Chen, J., Dong, J., Xia, Y., Liu, J. et al. (2015) Plasma miRNAs as early biomarkers for detecting hepatocellular carcinoma. *Int. J. Cancer* **137**, 1679–1690, https://doi.org/10.1002/ijc.29544
17 Qadir, M.I. and Faheem, A. (2017) miRNA: A Diagnostic and Therapeutic Tool for Pancreatic Cancer. *Crit. Rev. Eukaryot. Gene Expr.* **27**, 197–204, https://doi.org/10.1615/CritRevEukaryotGeneExpr.2017019494
18 Xu, G., Cai, J., Wang, L., Jiang, L., Huang, J., Hu, R. et al. (2018) MicroRNA-30e-5p suppresses non-small cell lung cancer tumorigenesis by regulating USP22-mediated Sirt1/JAK/STAT3 signaling. *Exp. Cell Res.* **362**, 268–278, https://doi.org/10.1016/j.yexcr.2017.11.027
19 Laudato, S., Patil, N., Abba, M.L., Leupold, J.H., Benner, A., Gaiser, T. et al. (2017) P53-induced miR-30e-5p inhibits colorectal cancer invasion and metastasis by targeting ITGA6 and ITGB1. **141**, 1879–1890
20 Zhang, Z., Qin, H., Jiang, B., Chen, W., Cao, W., Zhao, X. et al. (2019) miR-30e-5p suppresses cell proliferation and migration in bladder cancer through regulating metadherin. *J. Cell. Biochem.* **120**, 15924–15932, https://doi.org/10.1002/jcb.28866
21 Association, W.M. (2009) Declaration of Helsinki. Ethical principles for medical research involving human subjects. *J. Indian Med. Assoc.* **107**, 403–405
22 Chen, J.P., Luan, Y., You, C.X., Chen, X.H., Luo, R.C. and Li, R. (2010) TRPM7 regulates the migration of human nasopharyngeal carcinoma cell by mediating Ca(2+) influx. *Cell Calcium* **47**, 425–432, https://doi.org/10.1016/j.ceca.2010.03.003
23 Livak, J.K. and Schmittgen, T.D. (2001) Analysis of relative gene expression using different real-time quantitative PCR and 2-△△CT method. *Acta Agronom. Sin.* 402–408
24 Ferlay, J., Soerjomataram, I., Dikshit, R., Eser, S., Mathers, C., Rebelo, M. et al. (2015) Cancer incidence and mortality worldwide: sources, methods and major patterns in GLOBOCAN 2012. *Int. J. Cancer* **136**, E359–E386, https://doi.org/10.1002/ijc.29210
25 Wei, K.R., Zheng, R.S., Zhang, S.W., Liang, Z.H., Li, Z.M. and Chen, W.Q. (2017) Nasopharyngeal carcinoma incidence and mortality in China, 2013. *Chin. J. Cancer* **36**, 90, https://doi.org/10.1186/s40880-017-0257-9
26 Yang, W. (2017) Preclinical advances in nasopharyngeal carcinoma treatment. *Cell Cycle (Georgetown, Tex)* **16**, 1015–1016, https://doi.org/10.1080/15384101.2017.1316441
27 Kavitha, N., Vijayarathna, S., Jothy, S.L., Oon, C.E., Chen, Y., Kanwar, J.R. et al. (2014) MicroRNAs: biogenesis, roles for carcinogenesis and as potential biomarkers for cancer diagnosis and prognosis. *Asian Pacific J. Cancer Prevent.* **15**, 7489–7497, https://doi.org/10.7314/APJCP.2014.15.18.7489
28 Ma, Y.X., Zhang, H., Li, X.H. and Liu, Y.H. (2018) MiR-30e-5p inhibits proliferation and metastasis of nasopharyngeal carcinoma cells by targeting USP22. *Eur. Rev. Med. Pharmacol. Sci.* **22**, 6342–6349
29 Kramer, N., Walzl, A., Unger, C., Rosner, M., Krupitza, G., Hengstschlager, M. et al. (2013) In vitro cell migration and invasion assays. *Mutat. Res.* **752**, 10–24, https://doi.org/10.1016/j.mrrev.2012.08.001
30 Duff, D. and Long, A. (2017) Roles for RACK1 in cancer cell migration and invasion. *Cell. Signal.* **35**, 250–255, https://doi.org/10.1016/j.cellsig.2017.03.005
31 Wang, T., Xu, L., Jia, R. and Wei, J. (2017) MiR-218 suppresses the metastasis and EMT of HCC cells via targeting SERBP1. *Acta Biochim. Biophys. Sin. (Shanghai)* **49**, 383–391, https://doi.org/10.1093/abbs/gmx017
32 Deng, L., Tang, J., Yang, H., Cheng, C., Lu, S., Jiang, R. et al. (2017) MTA1 modulated by miR-30e contributes to epithelial-to-mesenchymal transition in hepatocellular carcinoma through an ErbB2-dependent pathway. *Oncogene* **36**, 3976–3985, https://doi.org/10.1038/onc.2016.491
33 Rao, Y.M., Ji, M., Chen, C.H. and Shi, H.R. (2013) Effect of siRNA targeting MTA1 on metastasis malignant phenotype of ovarian cancer A2780 cells. *J. Huazhong Univ. Sci. Technol. Med. Sci. = Hua zhong ke ji da xue xue bao Yi xue Ying De wen ban = Huazhong keji daxue xuebao Yixue Yingdewen ban* **33**, 266–271, https://doi.org/10.1007/s11596-013-1109-8
34 Lee, M.H., Koh, D., Na, H., Ka, N.L., Kim, S., Kim, H.J. et al. (2018) MTA1 is a novel regulator of autophagy that induces tamoxifen resistance in breast cancer cells. *Autophagy* **14**, 812–824, https://doi.org/10.1080/15548627.2017.1388476
35 Song, Q., Zhang, H., Wang, M., Song, W., Ying, M., Fang, Y. et al. (2013) MTA1 promotes nasopharyngeal carcinoma growth in vitro and in vivo. *J. Exp. Clin. Cancer Res. : CR* **32**, 54
36 Yuan, T., Zhang, H., Liu, B., Zhang, Q., Liang, Y., Zheng, R. et al. (2014) Expression of MTA1 in nasopharyngeal carcinoma and its correlation with prognosis. *Med. Oncol.* **31**, 330, https://doi.org/10.1007/s12032-014-0330-z
37 Wang, G., Wang, S. and Li, C. (2017) MiR-183 overexpression inhibits tumorigenesis and enhances DDP-induced cytotoxicity by targeting MTA1 in nasopharyngeal carcinoma. *Tumour Biol.: J. Int. Soc. Oncodevelopment. Biol. Med.* **39**, 1010428317703825
38 Mendez, M.G., Kojima, S. and Goldman, R.D. (2010) Vimentin induces changes in cell shape, motility, and adhesion during the epithelial to mesenchymal transition. *FASEB J. : Off. Publication Feder. Am. Societies Exp. Biol.* **24**, 1838–1851, https://doi.org/10.1096/fj.09-151639
39 Wei, F., Wu, Y., Tang, L., He, Y., Shi, L., Xiong, F. et al. (2018) BPIFB1 (LPLUNC1) inhibits migration and invasion of nasopharyngeal carcinoma by interacting with VTN and VIM. *Br. J. Cancer* **118**, 233–247, https://doi.org/10.1038/bjc.2017.385
40 Sang, Y., Cheng, C., Zeng, Y.X. and Kang, T. (2018) Snail promotes metastasis of nasopharyngeal carcinoma partly by down-regulating TEL2. *Cancer Communications (London, England)* **38**, 58, https://doi.org/10.1186/s40880-018-0328-6
41 Li, Y., Yang, X., Du, X., Lei, Y., He, Q., Hong, X. et al. (2018) RAB37 Hypermethylation Regulates Metastasis and Resistance to Docetaxel-Based Induction Chemotherapy in Nasopharyngeal Carcinoma. *Clin. Cancer Res.: An Off. J. Am. Assoc. Cancer Res.* **24**, 6495–6508, https://doi.org/10.1158/1078-0432.CCR-18-0532
42 Du, Z.M., Hu, C.F., Shao, Q., Huang, M.Y., Kou, C.W., Zhu, X.F. et al. (2009) Upregulation of caveolin-1 and CD147 expression in nasopharyngeal carcinoma enhanced tumor cell migration and correlated with poor prognosis of the patients. *Int. J. Cancer* **125**, 1832–1841, https://doi.org/10.1002/ijc.24531